



Published in final edited form as:

Pediatr Res. 2014 February ; 75(2): 266–272. doi:10.1038/pr.2013.224.

Gestational diabetes induces alterations in the function of neonatal endothelial colony forming cells

Emily K. Blue^{1,2}, Robert DiGiuseppe¹, Ethel Derr-Yellin^{1,2}, Juan Carlos Acosta¹, S. Louise Pay², Helmut Hanenberg^{1,2,3}, Megan M. Schellinger⁴, Sara K. Quinney⁴, Julie A. Mund^{1,2,3}, Jamie Case^{1,2,3}, and Laura S. Haneline^{1,2,3,5,6}

¹Department of Pediatrics, Indiana University School of Medicine, Indianapolis, IN

²Herman B Wells Center for Pediatric Research, Indiana University School of Medicine, Indianapolis, IN

³Indiana University Simon Cancer Center, Indiana University School of Medicine, Indianapolis, IN

⁴Department of Obstetrics and Gynecology, Indiana University School of Medicine, Indianapolis, IN

⁵Department of Microbiology & Immunology, Indiana University School of Medicine, Indianapolis, IN

⁶Department of Cellular & Integrative Physiology, Indiana University School of Medicine, Indianapolis, IN

Abstract

Background—Children born to mothers with gestational diabetes mellitus (GDM) experience increased risk of developing hypertension, type 2 diabetes mellitus, and obesity. Disrupted function of endothelial colony forming cells (ECFCs) may contribute to this enhanced risk. The goal of this study was to determine if cord blood ECFCs from GDM pregnancies exhibit altered functionality.

Methods—ECFCs isolated from the cord blood of control and GDM pregnancies were assessed for proliferation, senescence, and Matrigel network formation. The requirement for p38MAPK in hyperglycemia-induced senescence was determined using inhibitor and overexpression studies.

Results—GDM ECFCs were more proliferative than control ECFCs. However, GDM ECFCs exhibited decreased network forming ability in Matrigel. Aging of ECFCs by serial passaging led to increased senescence and reduced proliferation of GDM ECFCs. ECFCs from GDM pregnancies were resistant to hyperglycemia-induced senescence compared to controls. In response to hyperglycemia, control ECFCs activated p38MAPK, which was required for

Users may view, print, copy, download and text and data- mine the content in such documents, for the purposes of academic research, subject always to the full Conditions of use: http://www.nature.com/authors/editorial_policies/license.html#terms

Corresponding author: Laura S. Haneline, 705 Riley Hospital Dr. RI 2618, Indianapolis, IN 46202, Phone: (317) 274-4885; Fax: (317) 274-8679, lhanelin@iu.edu.

Disclosure: The authors declare no conflicts of interest.

hyperglycemia-induced senescence. In contrast, GDM ECFCs had no change in p38MAPK activation under equivalent conditions.

Conclusion—Intrauterine exposure of ECFCs to GDM induces unique phenotypic alterations. The resistance of GDM ECFCs to hyperglycemia-induced senescence and decreased p38MAPK suggest that these progenitor cells have undergone changes to induce tolerance to a hyperglycemic environment.

INTRODUCTION

Gestational diabetes mellitus (GDM) is common and complicates approximately 5–10% of all pregnancies (1). Substantial rates of maternal and neonatal complications are associated with GDM. However, in addition to short-term neonatal morbidities, multiple studies demonstrate that offspring of mothers with GDM have an increased risk to develop several chronic diseases including hypertension, obesity, type 2 diabetes (T2DM) and the metabolic syndrome (2–5). Despite the evidence that exists linking prenatal exposure to GDM to several diseases later in life, the mechanism for disease pathogenesis is currently unknown.

Individuals with diabetes mellitus (DM) are at a high risk to develop micro- and macrovascular diseases, demonstrating that a diabetic environment promotes vascular injury (6). Endothelial dysfunction precedes the development of many vascular diseases (7). The repair of damaged endothelium requires intact function of progenitor cells that reside in vessel walls and that circulate in the peripheral blood (8,9). Studies in adults and adolescents with DM show that reduced numbers and altered function of circulating progenitors are associated with endothelial dysfunction (10,11). Given these observations, we hypothesize that fetal exposure to a diabetic environment accelerates the onset of endothelial dysfunction by altering endothelial progenitor quantity and function.

Studies by our lab and others have characterized highly proliferative circulating endothelial progenitor cells referred to as endothelial colony forming cells (ECFCs) (8,9,12,13). Previously, we demonstrated that ECFCs from the cord blood of infants born to women with pregestational DM have reduced colony formation, premature senescence, decreased proliferation, and decreased vessel forming ability compared to control cord blood ECFCs (13). Because ECFCs from neonates born to women with GDM are also exposed to the diabetic milieu *in utero*, we hypothesized that cord blood ECFCs from GDM pregnancies would also exhibit altered function.

RESULTS

ECFCs from GDM pregnancies exhibit increased proliferation and reduced tube formation

The ability of a single cell to form a visible colony *in vitro* is a key defining characteristic of progenitor cells. Therefore, ECFCs from the cord blood of control and GDM pregnancies were plated in limiting dilution assays to validate progenitor function via colony-forming ability. In contrast to our previous data with ECFCs from pregnancies complicated by pregestational DM (13), GDM and control ECFCs had similar colony formation frequencies, both from original cord blood samples (Figure 1a) and from established cell lines (Figure 1b). To determine whether intrauterine exposure to GDM altered ECFC function, *in vitro*

assays were performed to assess senescence by staining for senescence-associated β -galactosidase (SA- β -gal) (14), proliferation using 3H thymidine incorporation assays, and network-forming ability in Matrigel studies. Baseline levels of senescence were negligible in both GDM and control ECFCs (data not shown). However, proliferation of GDM exposed ECFCs was significantly increased compared to controls (Figure 1c).

To further examine ECFCs from GDM pregnancies for evidence of dysfunction, cells were plated on Matrigel extracellular matrix to assess their ability to form closed network structures *in vitro*. Compared to control ECFCs, GDM ECFCs made ~30% fewer closed networks (Figure 1d). Taken together, these findings are intriguing given that ECFCs from GDM pregnancies were hyperproliferative, yet had poor network formation in Matrigel studies. We questioned whether the enhanced proliferation observed in ECFCs from GDM pregnancies predisposes the cells to premature senescence.

Aging of cells to induce senescence can be modeled *in vitro* via serial replating. Therefore, we next asked whether higher passage GDM ECFCs retained their hyperproliferative state and/or became senescent. Serial replating of ECFCs from GDM pregnancies showed that these cells had a reduced proliferative response both to baseline and growth factor stimulated conditions. As is shown in Figure 2a, higher passage GDM ECFCs were no longer hyperproliferative and trended toward decreased proliferation. SA- β -gal assays confirmed that serial replating of GDM ECFCs enhanced senescence compared to controls (Figure 2b). The increase in proliferation of early passage GDM ECFCs may lead to subsequent premature senescence and reduced proliferation.

ECFCs from GDM pregnancies are resistant to hyperglycemia-induced senescence

Previously, we demonstrated that control ECFCs exhibit enhanced senescence when exposed to hyperglycemia *in vitro* (13). It is possible that ECFCs from GDM pregnancies also undergo senescence in response to hyperglycemia. Alternatively, since ECFCs from GDM pregnancies were exposed to hyperglycemia *in utero* and have no increase in baseline senescence, GDM ECFCs may have adapted to the deleterious effects of hyperglycemia. To determine whether ECFCs from GDM pregnancies undergo senescence following treatment with elevated glucose concentrations, control and GDM ECFCs were cultured in euglycemic (5 mmol/l glucose) and hyperglycemic conditions (10 or 15 mmol/l glucose). As shown in Figure 3a and similar to previous studies (13), treating control ECFCs with either 10 or 15 mmol/l glucose induced a greater frequency of senescent cells. However, exposing ECFCs from GDM pregnancies to hyperglycemia did not increase senescence, resulting in significantly lower senescence compared to control cells. In addition, culturing ECFCs in elevated glucose concentrations did not increase numbers of apoptotic or necrotic cells in control or GDM ECFCs (data not shown). These data indicate that GDM ECFCs are resistant to hyperglycemia-induced senescence and suggest that adaptive changes have occurred that protect from hyperglycemic stress.

Previous studies demonstrate that p38MAPK is required for hyperglycemia-induced senescence in adult endothelial progenitor cells (15,16). However, the role of p38MAPK in promoting senescence of neonatal ECFCs after hyperglycemic exposure is unknown. Therefore, our initial studies evaluated whether control ECFCs treated with either 10 or 15

mmol/l glucose increased p38MAPK activation. Hyperglycemic treatment of control ECFCs stimulated a dose-dependent increase in phosphorylated or active p38MAPK (Figures 3b–3c). To determine whether ECFC senescence was dependent on p38MAPK activation, control ECFCs were cultured with or without a p38MAPK inhibitor, SB203580, in euglycemic and hyperglycemic conditions. Inhibition of p38MAPK prevented hyperglycemia-induced senescence in control ECFCs (Figure 3d), supporting an integral role for this stress-activated pathway in regulating senescence of ECFCs.

Given that p38MAPK is required for hyperglycemia-induced senescence together with the observation that GDM ECFCs do not undergo senescence after hyperglycemic treatment, we speculated that activation of p38MAPK was impaired in ECFCs from GDM pregnancies. As is shown in Figure 3b and quantified in Figure 3c, high glucose treatment of ECFCs from GDM pregnancies did not increase p38MAPK phosphorylation. These results are consistent with the idea that p38MAPK is required for hyperglycemia to induce senescence in ECFCs and indicate that resistance of GDM ECFCs to hyperglycemia-induced senescence may be due to aberrant regulation of p38MAPK activation.

To confirm a role for the p38MAPK pathway in regulating senescence of ECFCs, mutant cDNAs of mitogen activated protein kinase kinase 6 (MKK6) were stably expressed in ECFCs using lentiviral transduction methods (17). MKK6 was chosen because it directly and specifically activates p38MAPK by phosphorylating residues in the activation loop (18). Initially, a control ECFC cell line was transduced with lentiviral vectors encoding either an empty vector, a constitutively active MKK6, or an inactive MKK6 construct. Western blotting confirmed MKK6 overexpression in cells transduced with lentiviruses encoding the mutant MKK6 cDNAs and verified increased phosphorylation of p38MAPK in cells overexpressing constitutively active MKK6 (Figure 4a). For subsequent studies, control and GDM ECFC cell lines expressing either the constitutively active or inactive MKK6 constructs were evaluated for senescence under standard culture conditions. Both control and GDM ECFCs expressing constitutively active MKK6 had increased senescent cells compared to ECFCs expressing inactive MKK6 (Figure 4b). Previous studies demonstrated that the molecule downstream of p38MAPK required for promoting a senescent cellular fate is p16^{INK4A}, a cyclin dependent kinase inhibitor (19). Therefore, we next examined transduced cells for p16^{INK4A} expression by RTPCR and Western blotting. In control and GDM ECFCs with increased p38MAPK activity, p16^{INK4A} expression was significantly elevated at the RNA and protein levels compared to controls expressing the inactive MKK6 mutant (Figures 4c–d). Collectively, these data support an important role for the p38MAPK pathway in regulating senescence of ECFCs as well as support aberrant regulation of p38MAPK in ECFCs from GDM pregnancies.

DISCUSSION

Infants exposed to either GDM or pregestational DM *in utero* are at increased risk to develop several chronic diseases, and in some cases, with onset of symptomatology during childhood (2–5). Increases in systolic blood pressure and adiposity can be detected as early as 3 years of age in children born to women with GDM (2). Furthermore, offspring of pregnancies complicated by either GDM or pregestational DM exhibit an enhanced risk for

childhood onset of elevated blood pressure, overt hypertension, T2DM, and obesity (3,5). These complications have immediate health consequences for individual children. Moreover, each of these morbidities constitutes a significant risk factor for eventual cardiovascular mortality. Thus, it is critical to identify underlying mechanisms involved in disease pathogenesis so that preventative measures can be instituted prospectively in children of mothers with DM.

Fetal exposure to an adverse intrauterine environment likely results in alterations in long-lived stem and progenitor cells, especially given the early acquisition of chronic diseases in offspring typically found in older adults. The model of stem and/or progenitor cell damage and subsequent dysfunction as a mechanism involved in vascular disease progression has been described previously (20,21). However, minimal data are reported to support this concept in the developmental origins of vascular disease. ECFCs, an important progenitor population critical for vascular homeostasis, circulate in adult peripheral blood but are highly enriched in the endothelium of vessel walls and in umbilical cord blood (8). Circulating levels of ECFCs are altered in patients with coronary artery disease and diabetic retinopathy (12,22,23). Healthy adolescents and young adults with T1DM have altered circulating levels of ECFCs and evidence of endothelial dysfunction (11). Importantly, pulmonary artery ECFCs from patients with pulmonary artery hypertension exhibit increased proliferation (24). Based on these previous studies correlating ECFC levels and function to vascular disease, ECFCs represent a novel and accessible progenitor population to study the effects of an adverse intrauterine environment.

Previously, to test this notion, we examined ECFCs harvested from pregnancies complicated by pregestational DM for functional impairments. Pregestational DM ECFCs had decreased colony formation, reduced proliferative capacity, increased basal senescence, and profound deficiencies in vasculogenesis (13). In the current studies, we examined whether ECFCs from GDM pregnancies would be less dysfunctional since GDM is often associated with milder diabetic symptoms for a shorter duration as compared to pregestational DM (25). While several progenitor phenotypes examined support this concept (i.e. normal colony formation, normal baseline senescence, and modest reduction in tube forming ability), an unexpected finding was baseline hyperproliferation of GDM ECFCs. We speculate that this observation may reflect an adaptive response of ECFCs following intrauterine exposure to a GDM environment. However, increased proliferation was only transient. Passaging of GDM ECFCs led to decreased proliferative responses and premature senescence, which are remarkably similar to phenotypes observed in ECFCs from pregnancies complicated by type 1 and type 2 DM. It is possible that ECFCs exposed to pregestational DM may also exhibit a compensatory period of hyperproliferation. Due to the greater severity and/or longer exposure to the intrauterine DM environment, neonatal ECFCs harvested from pregestational DM pregnancies may have already progressed toward reduced proliferation and enhanced senescence. Future studies in animal models could be used to test this hypothesis, given the lack of feasibility in evaluating fetal ECFCs from human subjects.

Another adaptation identified in GDM ECFCs was resistance to hyperglycemia-induced senescence. The tolerance to hyperglycemia likely occurs through a signaling alteration involving p38MAPK, which is activated and required for senescence of control ECFCs.

GDM ECFCs treated with hyperglycemia did not activate p38MAPK, allowing the cells to resist senescence and to continue proliferating in the presence of elevated glucose concentrations. GDM ECFCs were capable of phosphorylating p38MAPK and undergoing senescence when an upstream activating molecule, MKK6, was expressed. Together these data support dysregulation of p38MAPK activity in ECFCs from GDM pregnancies, rather than an intrinsic defect in the ability of the ECFCs to undergo senescence. Though further studies are needed to elucidate the underlying mechanism responsible for aberrant p38MAPK regulation, our data identified novel cellular and biochemical adaptations in a primary neonatal progenitor population after *in vivo* GDM exposure. Our findings and approach have advantages compared to previous studies that examined biochemical and molecular alterations of endothelial cells treated with hyperglycemia *in vitro* (16,26,27) since the neonatal impact of GDM exposure is challenging to model *in vitro* or to replicate in animal models. This is due to the complexity of GDM, which involves maternal insulin resistance, beta-cell dysfunction, hyperlipidemia, and inflammation resulting in fetal hyperglycemia, hyperinsulinemia, and presumably additional metabolic consequences yet to be identified (28). Therefore, studying ECFCs after *in vivo* GDM exposure enhances physiologic relevance and provides unique insight into the long-term effects of the overall diabetic milieu on a neonatal progenitor cell population.

METHODS

Cord blood sample collection

Umbilical cord blood samples were collected from healthy, control pregnancies and pregnancies complicated by GDM after informed consent was obtained from the mothers. All pregnancies were singleton gestations. GDM was defined according to the American College of Obstetrics and Gynecology guidelines (29). All control subjects had a normal 50-gram oral glucose screen. Women with preeclampsia or hypertension were excluded as were women with other illnesses known to affect glucose metabolism or taking medications known to affect glucose metabolism. In addition, infants with known chromosomal abnormalities were excluded. The Institutional Review Board at the Indiana University School of Medicine approved this protocol. Pertinent health information is included for women (Table 1) and infants (Table 2) enrolled in the study.

ECFC culture and isolation

ECFCs were isolated from cord blood samples by the Indiana University Simon Cancer Center's Angiogenesis, Endothelial and Pro-Angiogenic Cell Core (AEPCC) as previously described (13,30). For routine culture of ECFCs, cells were grown in EGM2 (Lonza, Walkersville, MD) containing 10% FCS (Thermo Scientific Hyclone, Logan, UT). EGM2 is euglycemic (5 mmol/l). For hyperglycemia experiments, ECFCs were cultured in EGM2 supplemented with glucose to achieve concentrations of 10 or 15 mmol/l. Early passage ECFCs (less than passage 5) were used in all experiments, except where late passage ECFCs are indicated (passage 7).

Colony Formation Assays

Each assay was performed in triplicate, plating 200 cells per well as described (13). Average counts of total colonies from 5–7 cell lines from control and GDM groups are shown.

³H-Thymidine Incorporation Assay

Studies were performed as previously described (13). ECFCs were incubated in EBM2 containing 5% FCS overnight and then plated in triplicate at 50,000 cells per well of a 6-well plate in EBM2 with 1% FCS for 16 hours. ECFCs were then cultured in serum-free EBM2 for 8 hours to induce quiescence. Proliferation was induced by addition of 2% FCS for 16 hours. Cells were pulsed with 1 μ Ci ³H-thymidine (Perkin-Elmer, Boston, MA) for 5 hours, washed, and then lysed in 0.1M NaOH. Incorporated ³H-thymidine was quantified on a liquid scintillation counter for triplicate wells. Average counts in 4 independent experiments were normalized to values obtained from control cells.

Senescence-Associated Beta-Galactosidase (SA- β -gal) Staining

ECFCs were cultured in EGM2 containing the indicated concentration of glucose for 7 days. Staining was performed as described (13,14). Triplicate wells were plated for all conditions. At least 100 total cells per well were scored, and the average percentage of SA- β -gal positive cells was determined per sample. Senescence was quantified for *in vitro* aged cells in 3 independent experiments and following hyperglycemia in 4 independent experiments.

Matrigel Assay

Tube forming ability on Matrigel was conducted as described (13). Briefly, 96-well plates were coated with 50 μ l Matrigel (Becton Dickinson, Franklin Lakes, NJ). ECFCs were plated on in triplicate at a density of 5000 cells per well in EGM2. After incubating at 37°C for 16 hours, phase contrast images were taken using a Spot camera (Spot Imaging Solutions, Sterling Heights, MI) on an Axiovert 35 microscope (Zeiss, Thornwood, NY). The number of closed networks per well was scored. Triplicate measurements were averaged for each of 4 cell lines per group.

Western blotting

Cells were lysed in RIPA buffer containing Complete Protease Inhibitor Cocktail (Roche Applied Science, Indianapolis, IN). Equal protein amounts were separated by gel electrophoresis on precast gels (Life Technologies, Grand Island, NY). Protein was transferred to nitrocellulose, and immunoblotted with antibodies to either phosphorylated-p38MAPK, total p38MAPK, MKK6, (Cell Signaling Technology, Beverly, MA), p16^{INK4a} (ab81278, Abcam, Cambridge, MA), or β -actin (Sigma-Aldrich Inc., St. Louis, MO). Secondary antibodies conjugated to HRP were from Biorad (Hercules, CA). Blots were developed with Pierce Supersignal West Pico (ThermoFisher, Hanover Park, IL), exposed to film, scanned and compiled in Photoshop CS5.1 (Adobe, San Jose, CA). Band intensity was quantified using ImageJ (NIH, Bethesda, MD). Graphs of semi-quantitative data were generated on 3–6 cell lines per group.

Generation of lentivirus encoding recombinant MKK6 cDNA constructs

Plasmids containing cDNA for a constitutively active mitogen activated protein kinase kinase 6 (MKK6 Glu; Addgene plasmid 13518) or kinase inactive MKK6 (K82A; Addgene plasmid 13519) were a generous gift from Dr. Roger Davis (18). The cDNAs were subcloned into the lentiviral vector (pUC2CL6IPwo), which was obtained from Dr. Helmut Hanenberg (17). The lentiviral vector contains a puromycin resistance gene to enable selection of transduced cells. Lentivirus was produced by co-transfection of HEK-293T cells with a lentiviral vector, packaging plasmid pCD/NL-BH, and VSV-G envelope plasmid using Fugene 6 (Roche, Indianapolis, IN). Lentivirus-containing supernatants were then collected, filtered through an 0.45 μ M asymmetric polyethersulfone filter unit (Thermo Scientific, Waltham, MA), and stored at -80°C .

Lentiviral transduction of ECFCs

ECFCs were plated at 25,000 cells per well in a 6-well tissue culture dish the day prior to transduction. Lentiviral vector supernatant was added to each well at a dilution of 1:5–1:10, in a final volume of 1mL of EGM2 + 10% FCS containing 21 μ M (8 μ g/mL) Polybrene (Sigma, St. Louis, MO), and incubated overnight. Media was changed, and plates were then incubated for 48h. Transduced cells were selected in media containing 1.8 μ M (1 μ g/mL) puromycin (Life Technologies, Grand Island, NY) for 2 days or until no live cells remained in the selection control plate. Protein lysates were obtained as described, and MKK6 expression and phosphorylated p38MAPK levels were confirmed for each transduction by western blotting.

Real-time RT-PCR

ECFCs were lysed in Qiazol (Qiagen, Valencia, CA), and RNA was obtained using manufacturer's instructions. RNA was reverse transcribed using a Transcriptor Universal cDNA Master Kit (Roche). RTPCR was performed on a Lightcycler 480 (Roche). For detection of p16^{INK4a}, a Universal Probe Master mix was used with Probe #34 from the Roche Universal Probe Library, and p16^{INK4a} primers (5'-GTGGACCTGGCTGAGGAG-3' and 5'-CTTTCAATCGGGGATGTCTG-3'). HPRT was used to normalize p16^{INK4a} values using the 2^{-C_t} method. Detection of HPRT was performed using Lightcycler 480 SYBR Green I Master Mix (Roche) and HPRT primers: 5'-CCTTGGTCAGGCAGTATAATCCA-3'; 5'-GGTCCTTTTCACCAGCAAGCT-3').

Statistical analysis

Data illustrated are mean \pm SEM. Two-way ANOVAs, followed by Sidak's multiple comparisons or Kruskal-Wallis one-way ANOVAs were performed on comparisons of more than two groups, as indicated in the figure legends. Unpaired t-tests were conducted when only two groups were compared and data were normally distributed. Prism 6 (GraphPad Software, La Jolla, CA) was used for all statistical analyses, and significance was noted when $p < 0.05$.

ACKNOWLEDGMENTS

The authors gratefully acknowledge research nurse Lucy Miller for assisting with cord blood collection. We thank Emily Sims and the Indiana University Simon Cancer Center's Angiogenesis, Endothelial and Pro-Angiogenic Cell Core (AEPCC) for the processing and culture of the ECFCs from umbilical cord blood. We also thank Elizabeth Rybak for providing excellent administrative support.

Statement of financial support: U.S. Public Health Services grants R01 HL094725 (L.S.H.), P30 CA82709 (L.S.H.), U10 HD063094 (L.S.H. and S.Q.) P30 DK090948 CEMH (J.C.), CA138237-01 (H.H.), and CA155294-01 (H.H.); and the Riley Children's Foundation, Indianapolis, IN (L.S.H.).

REFERENCES

1. Metzger BE, Buchanan TA, Coustan DR, et al. Summary and recommendations of the Fifth International Workshop-Conference on Gestational Diabetes Mellitus. *Diabetes Care*. 2007; 30(Suppl 2):S251–S260. [PubMed: 17596481]
2. Wright CS, Rifas-Shiman SL, Rich-Edwards JW, Taveras EM, Gillman MW, Oken E. Intrauterine exposure to gestational diabetes, child adiposity, and blood pressure. *Am J Hypertens*. 2009; 22:215–220. [PubMed: 19023272]
3. Boney CM, Verma A, Tucker R, Vohr BR. Metabolic syndrome in childhood: association with birth weight, maternal obesity, and gestational diabetes mellitus. *Pediatrics*. 2005; 115:e290–e296. [PubMed: 15741354]
4. Bunt JC, Tataranni PA, Salbe AD. Intrauterine exposure to diabetes is a determinant of hemoglobin A(1)c and systolic blood pressure in pima Indian children. *J Clin Endocrinol Metab*. 2005; 90:3225–3229. [PubMed: 15797952]
5. Cho NH, Silverman BL, Rizzo TA, Metzger BE. Correlations between the intrauterine metabolic environment and blood pressure in adolescent offspring of diabetic mothers. *J Pediatr*. 2000; 136:587–592. [PubMed: 10802488]
6. Winer N, Sowers JR. Epidemiology of diabetes. *J Clin Pharmacol*. 2004; 44:397–405. [PubMed: 15051748]
7. Avogaro A, Albiero M, Menegazzo L, de Kreutzenberg S, Fadini GP. Endothelial dysfunction in diabetes: the role of reparatory mechanisms. *Diabetes Care*. 2011; 34(Suppl 2):S285–S290. [PubMed: 21525470]
8. Ingram DA, Mead LE, Moore DB, Woodard W, Fenoglio A, Yoder MC. Vessel wall-derived endothelial cells rapidly proliferate because they contain a complete hierarchy of endothelial progenitor cells. *Blood*. 2005; 105:2783–2786. [PubMed: 15585655]
9. Ingram DA, Mead LE, Tanaka H, et al. Identification of a novel hierarchy of endothelial progenitor cells using human peripheral and umbilical cord blood. *Blood*. 2004; 104:2752–2760. [PubMed: 15226175]
10. Georgescu A. Vascular dysfunction in diabetes: The endothelial progenitor cells as new therapeutic strategy. *World J Diabetes*. 2011; 2:92–97. [PubMed: 21860692]
11. DiMeglio LA, Tosh A, Saha C, et al. Endothelial abnormalities in adolescents with type 1 diabetes: a biomarker for vascular sequelae? *J Pediatr*. 2010; 157:540–546. [PubMed: 20542287]
12. Guven H, Shepherd RM, Bach RG, Capoccia BJ, Link DC. The number of endothelial progenitor cell colonies in the blood is increased in patients with angiographically significant coronary artery disease. *J Am Coll Cardiol*. 2006; 48:1579–1587. [PubMed: 17045891]
13. Ingram DA, Lien IZ, Mead LE, et al. In vitro hyperglycemia or a diabetic intrauterine environment reduces neonatal endothelial colony-forming cell numbers and function. *Diabetes*. 2008; 57:724–731. [PubMed: 18086900]
14. van der Loo B, Fenton MJ, Erusalimsky JD. Cytochemical detection of a senescence-associated beta-galactosidase in endothelial and smooth muscle cells from human and rabbit blood vessels. *Exp Cell Res*. 1998; 241:309–315. [PubMed: 9637772]
15. Kuki S, Imanishi T, Kobayashi K, Matsuo Y, Obana M, Akasaka T. Hyperglycemia accelerated endothelial progenitor cell senescence via the activation of p38 mitogen-activated protein kinase. *Circ J*. 2006; 70:1076–1081. [PubMed: 16864945]

16. Chen YH, Lin SJ, Lin FY, et al. High glucose impairs early and late endothelial progenitor cells by modifying nitric oxide-related but not oxidative stress-mediated mechanisms. *Diabetes*. 2007; 56:1559–1568. [PubMed: 17389326]
17. Nakano M, Kelly EJ, Wiek C, Hanenberg H, Rettie AE. CYP4V2 in Bietti's crystalline dystrophy: ocular localization, metabolism of omega-3-polyunsaturated fatty acids, and functional deficit of the p.H331P variant. *Mol Pharmacol*. 2012; 82:679–686. [PubMed: 22772592]
18. Raugeaud J, Whitmarsh AJ, Barrett T, Derijard B, Davis RJ. MKK3- and MKK6-regulated gene expression is mediated by the p38 mitogen-activated protein kinase signal transduction pathway. *Mol Cell Biol*. 1996; 16:1247–1255. [PubMed: 8622669]
19. Lowe SW, Sherr CJ. Tumor suppression by Ink4a-Arf: progress and puzzles. *Curr Opin Genet Dev*. 2003; 13:77–83. [PubMed: 12573439]
20. Olivieri F, Recchioni R, Marcheselli F, et al. Cellular senescence in cardiovascular diseases: potential age-related mechanisms and implications for treatment. *Curr Pharm Des*. 2013; 19:1710–1719. [PubMed: 23061728]
21. Minamino T, Komuro I. Vascular aging: insights from studies on cellular senescence, stem cell aging, and progeroid syndromes. *Nat Clin Pract Cardiovasc Med*. 2008; 5:637–648. [PubMed: 18762784]
22. Tan K, Lessieur E, Cutler A, et al. Impaired function of circulating CD34(+) CD45(–) cells in patients with proliferative diabetic retinopathy. *Exp Eye Res*. 2010; 91:229–237. [PubMed: 20493838]
23. Meneveau N, Deschaseaux F, Seronde MF, et al. Presence of endothelial colony-forming cells is associated with reduced microvascular obstruction limiting infarct size and left ventricular remodelling in patients with acute myocardial infarction. *Basic Res Cardiol*. 2011; 106:1397–1410. [PubMed: 21904841]
24. Duong HT, Comhair SA, Aldred MA, et al. Pulmonary artery endothelium resident endothelial colony-forming cells in pulmonary arterial hypertension. *Pulm Circ*. 2011; 1:475–486. [PubMed: 22530103]
25. Gestational diabetes mellitus. *Diabetes Care*. 2004; 27(Suppl 1):S88–S90. [PubMed: 14693936]
26. El-Osta A, Brasacchio D, Yao D, et al. Transient high glucose causes persistent epigenetic changes and altered gene expression during subsequent normoglycemia. *J Exp Med*. 2008; 205:2409–2417. [PubMed: 18809715]
27. Brasacchio D, Okabe J, Tikellis C, et al. Hyperglycemia induces a dynamic cooperativity of histone methylase and demethylase enzymes associated with gene-activating epigenetic marks that coexist on the lysine tail. *Diabetes*. 2009; 58:1229–1236. [PubMed: 19208907]
28. Hollingsworth DR. Alterations of maternal metabolism in normal and diabetic pregnancies: differences in insulin-dependent, non-insulin-dependent, and gestational diabetes. *Am J Obstet Gynecol*. 1983; 146:417–429. [PubMed: 6344640]
29. ACOG Practice Bulletin. Clinical management guidelines for obstetrician-gynecologists. Gestational diabetes. *Obstet Gynecol*. 2001; 98:525–538. Number 30, September 2001 (replaces Technical Bulletin Number 200, December 1994). [PubMed: 11547793]
30. Mead LE, Prater D, Yoder MC, Ingram DA. Isolation and characterization of endothelial progenitor cells from human blood. *Curr Protoc Stem Cell Biol*. 2008; Chapter 2(Unit 2C 1)

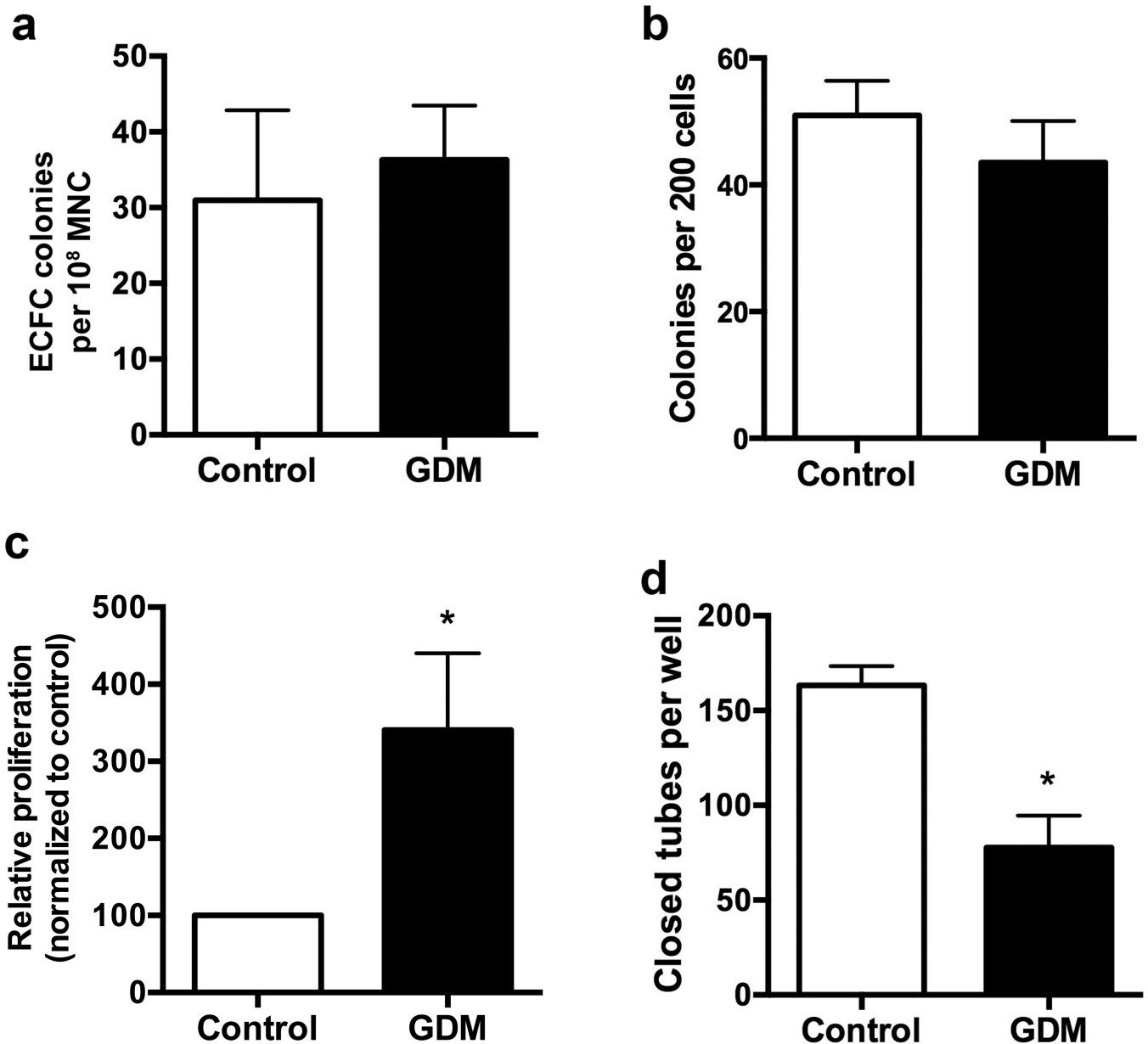


Figure 1. GDM ECFCs exhibit increased proliferation and impaired tube forming ability
(a) Frequency of ECFC colonies per 10^8 cord blood mononuclear cells (MNC). Approximately 2×10^8 MNC were plated on collagen-coated plates. Colonies were counted between days 10–14. Frequency of ECFCs was calculated by normalizing to cell number plated for each sample, $n=5$ for control and $n=7$ for GDM samples. **(b)** Frequency of ECFC colonies in limiting dilution assays. Colonies were scored by visual inspection after 7 days in culture, $n=6$ per group. **(c)** ^3H -Thymidine incorporation assay to assess proliferation. Relative proliferation was calculated by dividing the scintillation count for individual culture conditions by the baseline value for control ECFCs then multiplying by 100. Results are from 7 independent experiments using 5–6 different cell lines per group. White bars indicate control ECFCs, and black bars indicated GDM ECFCs. * $p<0.05$ by Wilcoxon signed rank

test. **(d)** Network formation in Matrigel. ECFCs were plated in Matrigel for 16 hours. Images were obtained and total closed networks per well were quantified, n=4 per group, *p<0.05 compared to control by unpaired t test.

Author Manuscript

Author Manuscript

Author Manuscript

Author Manuscript

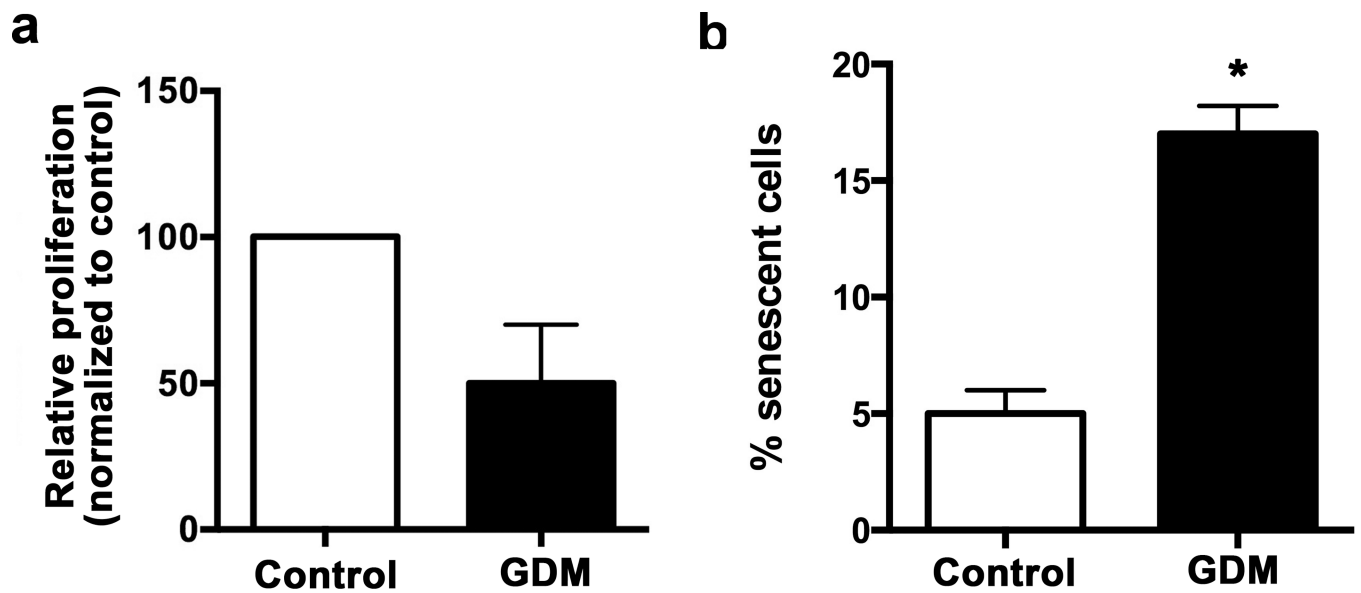


Figure 2. Serial passage of ECFCs from GDM pregnancies decreased proliferation and increased senescence

(a) ^3H -Thymidine incorporation assay to assess proliferation as described previously (13). Relative proliferation was calculated by dividing the scintillation count for individual culture conditions by the baseline value for control ECFCs then multiplying by 100, $n=4$. White bars indicate control ECFCs, and black bars indicated GDM ECFCs. Serial passaged GDM ECFCs were no longer more proliferative than similarly passaged control ECFCs (not significant by unpaired t test). (b) Senescence after serial passage. Frequency of SA- β -gal positive cells was measured in passage 7 ECFCs, $n=3$, $*p<0.05$ by unpaired t test.

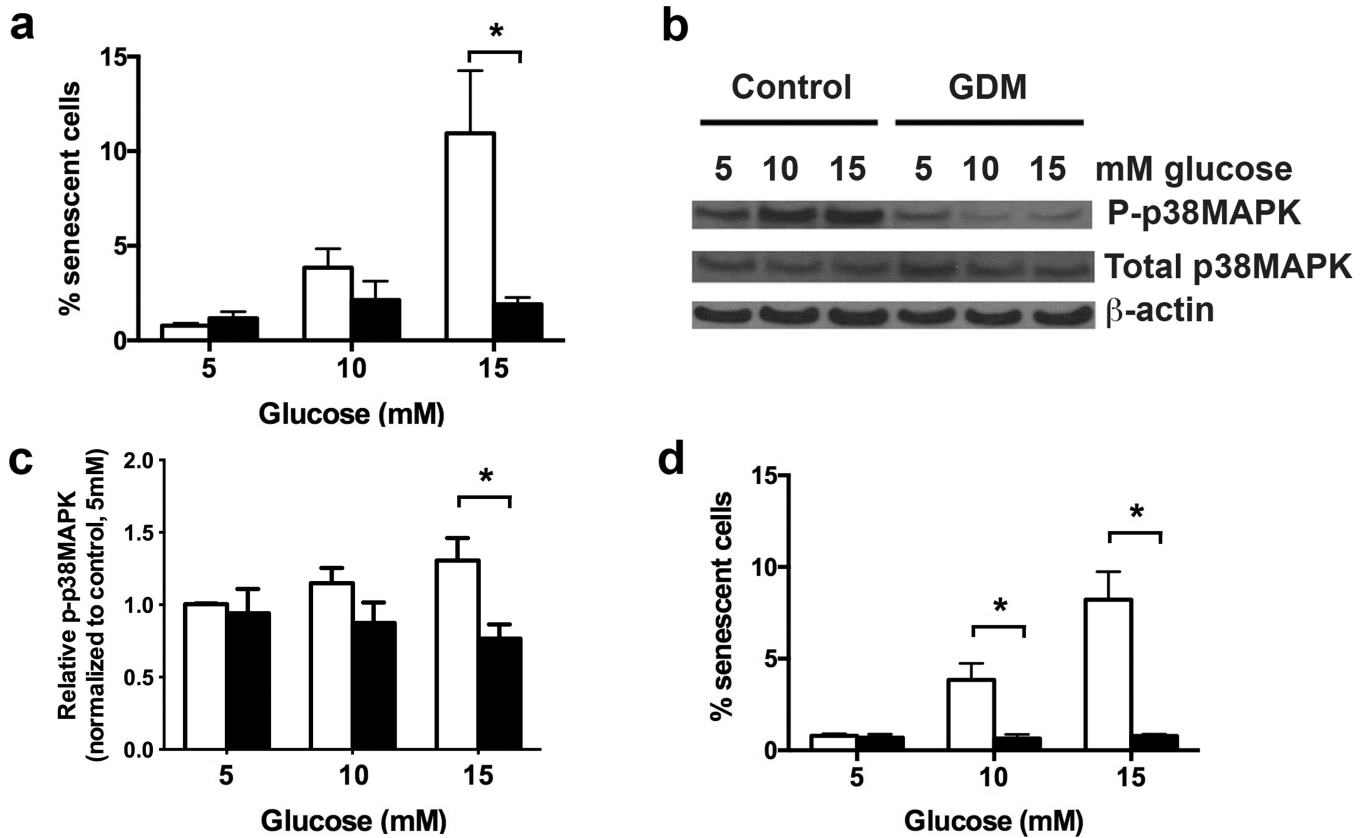


Figure 3. Hyperglycemic treatment of GDM ECFCs did not induce senescence or activate p38MAPK

(a) Hyperglycemia-induced senescence. ECFCs were plated in EGM2 containing the indicated glucose concentration for 7 days. The percentage of SA- β -gal positive cells was calculated in 4 independent experiments. White bars indicate control ECFCs, and black bars indicated GDM ECFCs. Two-way ANOVA determined a significant increase in senescence by hyperglycemia, and with significantly less senescence in GDM ECFCs. * $p < 0.05$ by Sidak's multiple comparison. (b) Hyperglycemia induced p38MAPK phosphorylation in ECFCs. Western blotting was performed on lysates from control ECFCs treated with indicated glucose concentrations to detect phospho-p38MAPK and total p38MAPK. β -actin was used as a loading control. (c) Quantitation of band intensity from Western blots in panel (b) in 6 independent experiments. Bands were quantified in ImageJ. Phospho-p38MAPK (P-p38MAPK) levels were normalized to total p38MAPK. A significant increase in p38MAPK phosphorylation with higher glucose concentration was found by 2-way ANOVA. Decreased phospho-p38MAPK was found in GDM ECFCs as indicated (* $p < 0.05$) by Sidak's multiple comparisons. (d) Effect of p38MAPK inhibition on senescence. Control ECFCs were cultured in 5, 10, or 15 mmol/l glucose with or without 1 μ M of the p38MAPK inhibitor, SB203580. White bars indicate control ECFCs, and black bars indicated GDM ECFCs. After 7 days, the percentage of SA- β -gal positive cells was quantified. Results are from 4 independent experiments. SB203580 significantly decreased senescence, with * $p < 0.05$ as indicated (two-way ANOVA followed by Sidak's multiple comparisons).

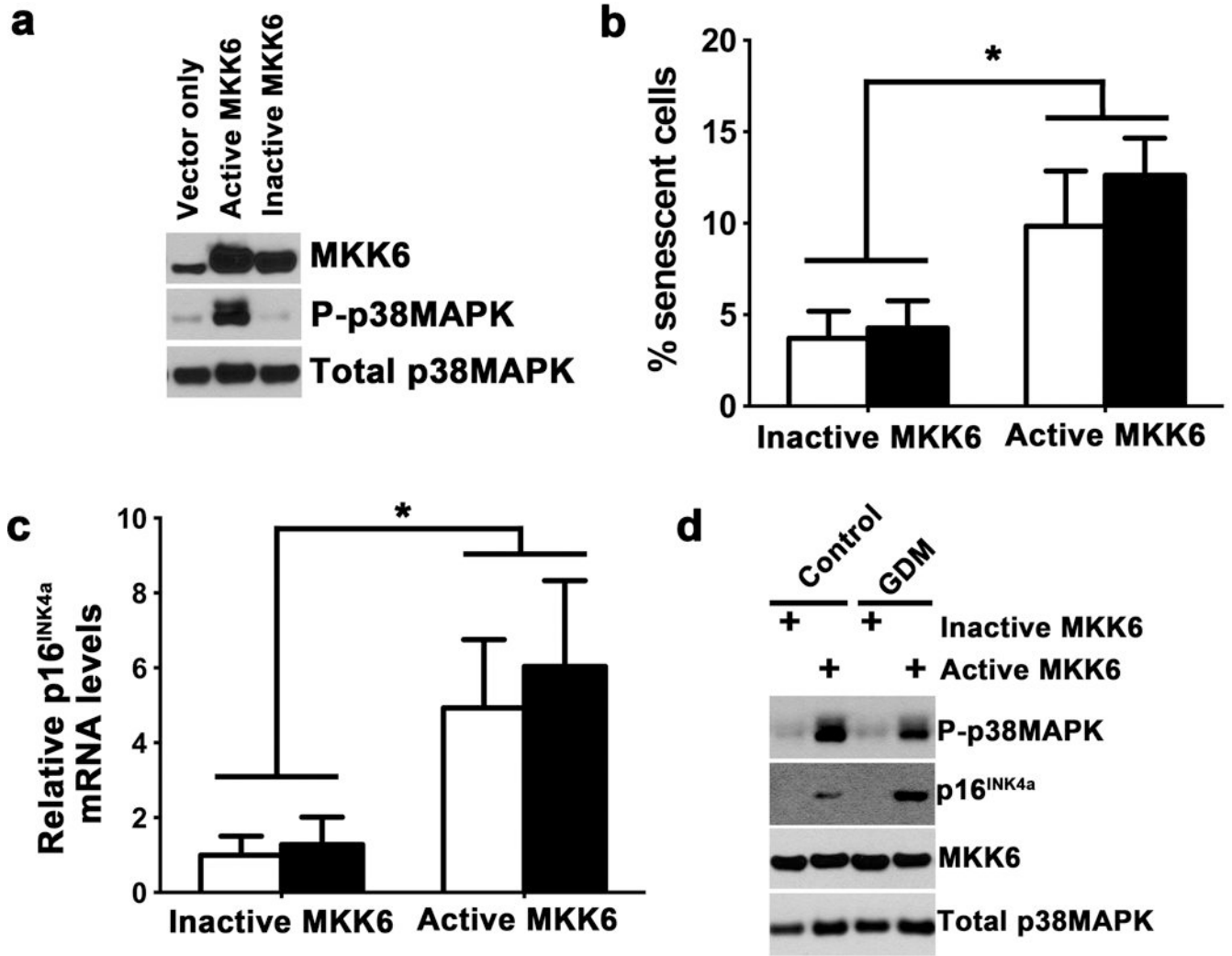


Figure 4. Activation of p38MAPK in ECFCs induces senescence and p16 expression
 (a) Overexpression of active MKK6 by lentiviral transduction in control ECFCs increases phospho-p38MAPK. Control ECFCs were also transduced by lentivirus expressing empty vector or kinase inactive MKK6. Western blotting of lysates confirmed increased phospho-p38MAPK by active MKK6, but not empty vector or inactive MKK6. Blot is representative of 3 independent experiments. (b) Effect of p38MAPK activation by active MKK6 on senescence in control and GDM ECFCs. Following transduction with either active or inactive MKK6, the percentage of SA-β-gal positive control and GDM ECFCs was assessed. White bars indicate control ECFCs, and black bars indicated GDM ECFCs. Expression of active MKK6 induced significantly increased senescence in both control and GDM ECFCs, by two-way ANOVA (* $p < 0.05$). No differences between control and GDM were found by Sidak's multiple comparisons. Results shown are from 3 independent experiments. (c) p16^{INK4a} expression is increased following expression of active MKK6, but not inactive MKK6. RNA was isolated from control and GDM ECFCs overexpressing active or inactive MKK6. Relative mRNA levels of p16^{INK4a} were quantified by real-time RTPCR, normalizing to HPRT expression. White bars indicate control ECFCs, and black bars

indicate GDM ECFCs. Two-way ANOVA identified a significant increase in p16^{INK4a} mRNA in ECFCs overexpressing active MKK6 compared to ECFCs expressing inactive MKK6 (*p<0.05). No significant difference was found between control and GDM. Results represent 3 different cell lines from both control and GDM groups. (d) Western blotting confirmed increased expression of p16^{INK4a} with active MKK6 and p38MAPK activation (P-p38MAPK). Total p38MAPK is shown as a loading control. Blots are representative of 3 independent experiments.

Author Manuscript

Author Manuscript

Author Manuscript

Author Manuscript

Table 1

Clinical data for maternal subjects

	Maternal age (years)	Medications	Maternal prepregnancy BMI	HbA1c
Control 1	26	Penicillin	48	ND
Control 2	38	None	28	ND
Control 3	26	None	44	ND
Control 4	37	None	37	ND
Control 5	42	None	35	ND
Control 6	24	Zoloft	19	ND
GDM 1	32	None	31	5.8
GDM 2	28	Insulin	27	6.4
GDM 3	24	None	44	6.2
GDM 4	25	None	37	ND
GDM 5	41	Penicillin	34	5.9
GDM 6	33	Glyburide, Zoloft	39	5.6
GDM 7	37	None	20	5.7

ND=not done

Table 2

Clinical data for infant subjects

	Sex	Gestational age (weeks complete)	Infant weight (kg)	Infant weight percentile*	Infant weight/length percentile*
Control 1	Male	38	3.10	10–25%	25%
Control 2	Female	40	3.38	25–50%	10–25%
Control 3	Male	41	3.98	75–90%	25–50%
Control 4	Male	39	3.70	50–75%	10–25%
Control 5	Female	38	2.91	10–25%	5–10%
Control 6	Female	40	3.45	50–75%	90–95%
GDM 1	Male	38	4.06	75–90%	50%
GDM 2	Female	39	4.18	95–97%	95–97%
GDM 3	Female	39	3.76	75–90%	75–90%
GDM 4	Male	37	3.09	10–25%	5%
GDM 5	Female	39	3.21	25–50%	25%
GDM 6	Male	39	3.61	50–75%	50–75%
GDM 7	Female	38	3.47	50–75%	25–50%

* Percentiles obtained from CDC 2000 Clinical Growth Charts (http://www.cdc.gov/growthcharts/clinical_charts.htm).